

https://dspace.org/

Hydrometallurgical Leaching of Copper and Cobalt from a CopperCobalt ore by Aqueous Choline ChlorideBased Deep Eutectic Solvent Solutions

Emmanuel Oke; Yorkabel Fedai; Johannes Potgieter

MDPI AG
https://hdl.handle.net/10539/46816
WOS

Downloaded from a DSpace repository. https://dspace.org/

minerals

MDPI

Article

Hydrometallurgical Leaching of Copper and Cobalt from a Copper–Cobalt Ore by Aqueous Choline Chloride-Based Deep Eutectic Solvent Solutions

Emmanuel Anuoluwapo Oke, Yorkabel Fedai and Johannes Hermanus Potgieter *

Sustainable and Innovative Minerals and Metals Extraction Technology (SIMMET) Research Group, School of Chemical and Metallurgical Engineering, University of the Witwatersrand, Private Bag X3 PO Wits 2050, Johannesburg 2050, South Africa; emmanuel.oke@wits.ac.za (E.A.O.); yorkabelgfedai@gmail.com (Y.F.)
* Correspondence: herman.potgieter@wits.ac.za

Abstract

The sustainable recovery of valuable metals such as Cu and Co from ores is a pressing need considering environmental and economic challenges. Therefore, this study evaluates the effectiveness of deep eutectic solvents (DESs) as alternative leaching agents for Cu and Co extraction. Four DESs were prepared using choline chloride (ChCl) as a hydrogen bond acceptor (HBA) and oxalic acid (OA), ethylene glycol (EG), urea (U) and thiourea (TU) as hydrogen bond donors (HBDs). Leaching experiments were conducted with DESs supplemented with 30 wt.% water at varying temperatures, various solid-to-liquid ratios, and time durations. The ChCl:OA DES demonstrated the highest leaching efficiencies among the DESs tested on pure CuO and CoO, achieving 89.2% for Cu and 92.4% for Co (60 °C, 400 rpm, 6 h, −75 + 53 µm particle size, and 1:10 solid-to-liquid ratio). In addition, the dissolution kinetics, analysed using the shrinking core model (SCM), showed that the leaching process was mainly controlled by surface chemical reactions. The activation energy values for Cu and Co leaching were 46.8 kJ mol^{-1} and 51.4 kJ mol^{-1}, respectively, supporting a surface chemical control mechanism. The results highlight the potential of ChCl:OA as a sustainable alternative for metal recovery.

Keywords: resource recovery; metals; dissolution kinetics; shrinking core model; activation energy

check for updates

Academic Editor: Qicheng Feng

Received: 3 July 2025
Revised: 28 July 2025
Accepted: 30 July 2025
Published: 31 July 2025

Citation: Oke, E.A.; Fedai, Y.; Potgieter, J.H. Hydrometallurgical Leaching of Copper and Cobalt from a Copper–Cobalt Ore by Aqueous Choline Chloride-Based Deep Eutectic Solvent Solutions. *Minerals* **2025**, *15*, 815. https://doi.org/10.3390/min15080815

Copyright: © 2025 by the authors. Licensee MDPI, Basel, Switzerland. This article is an open access article distributed under the terms and conditions of the Creative Commons Attribution (CC BY) license (https://creativecommons.org/licenses/by/4.0/).

1. Introduction

Given how crucial the mining and exploration industries are to the supply of primary metals, it is concerning when reserves of ores with high metallic values decline. A staggering 22 million tons of Cu are needed each year, making it a highly sought-after metal globally [1]. The manufacturing of electronics, power grids, transportation, and construction are just a few of the industries that demonstrate their versatility. Cu is renowned for its exceptional conductivity for heat and electricity, outstanding corrosion resistance, flexibility and pliability [2]. Sulphide minerals (chalcopyrite, bornite, covellite, chalcocite, etc.) make up most of the world's Cu reserves, while oxides make up a very small percentage [3]. Also, Co is an essential raw material that has been widely utilised in the manufacturing of batteries, alloys, catalysts, ceramics, and other materials because of its unique properties, which include temperature-dependent crystal structure, ferromagnetism, and corrosion resistance [4,5]. Co is arguably best known for its use as an electrode component in lithium-ion batteries. In 2020, 64.0% of the world's refined Co was used in battery production [6].

Global consumption of Co in 2021 was over 175,000 tons, up roughly 86.0% from the 93,950 tons consumed in 2016. Furthermore, it is anticipated that the demand for Co will increase dramatically by 2050 [7].

When choosing metal recovery techniques, factors like capital cost, energy use, and carbon footprint are important considerations [8]. Metals have long been extracted from ores using traditional techniques like hydrometallurgy and pyrometallurgy [9]. In the pyrometallurgical process, ores, concentrates, or alloys are heated to temperatures over the melting point of the final metal in order to extract or purify them. The high lattice energy and strong stability of metal oxides in pyrometallurgical processes necessitate high temperatures, often exceeding 1200 °C. Pyrometallurgy is becoming economically unjustified due to the growing demand for rare earth group metals and the complex materials that are a valuable source of them [10]. Interestingly, hydrometallurgical techniques can be used in conjunction with less energy-intensive pyrometallurgical techniques. Their suitability for processing raw materials with a lower metal content and a more complicated composition is a benefit. Stirring and percolation are the two leaching methods typically used in hydrometallurgy. A few drawbacks of hydrometallurgical processes include the requirement for several steps, the usage of a lot of chemicals, and the production of acidic and alkaline waste streams that need to be neutralised and treated before being disposed of [11,12]. Innovative techniques are needed to extract metals from difficult feedstocks, such as secondary urban mines or low-grade ores. There are several approaches which can be adopted for the different types of metal ores, such as oxides, sulphides, carbonates, phosphates, and silicates. Generally, oxide forms dissolve in strong basic or acidic solutions [13]. Other techniques for recovering metals include leaching with mineral acids, cementation, precipitation, and electrowinning. The final procedure, which often uses sulfuric acid, a cheap raw ingredient that is readily available in large amounts, is most pertinent. However, this method lacks selectivity, necessitates the use of large quantities of acid, and is rarely environmentally benign [5,9,14].

Solvometallurgy, also known as ionometallurgy, is a novel field of metallurgy that is comparable to hydrometallurgy in terms of working circumstances and unit operations. The distinction, however, is that solvometallurgy employs non-aqueous solvents, such as deep eutectic solvents (DESs), ionic liquids (ILs), and molecular organic solvents, instead of aqueous solutions of acids or bases. Solvometallurgy's primary advantages over conventional metallurgical processes are its increased selectivity and reduced water usage, which may be used to process low-grade ores [8,15]. Although ILs have been investigated for metal recovery, their industrial scalability is limited by toxicity, high cost, and complex synthetic routes that often require purification. In contrast, DESs are straightforward mixtures synthesised using easily accessible and reasonably priced compounds that provide tunability through changes in the molar ratio or constituent parts [16]. DESs are a combination of hydrogen bond acceptors (HBAs), primarily ammonium salts, and hydrogen bond donors (HBDs), typically alcohols, amides, and organic acids [16,17]. By adjusting the HBD or changing the molar ratio, it can be adjusted to optimise a specific property. Several studies in recent years have examined variables such as pH, water content, rheology, and HBD selection in relation to the application of DESs for metal oxide dissolution [18–20]. Metal selectivity and dissolution efficiency have been improved by fine-tuning parameters such as reaction time, temperature, and molar ratio, among others. A wide range of substances, such as urea (U), ethylene glycol (EG), and choline chloride (ChCl), have been thoroughly investigated for metal recovery procedures [21,22]. In DES constituted by U and ChCl, EG and ChCl, as well as malonic acid and ChCl at a 1:1 molar ratio, Abbott et al. examined the dissolving behaviour of several metal oxides [23]. The authors compared these DESs to

HCl in terms of metal solubility. They also investigated the solubility of transition metal oxides by employing oxalic acid and EG as solvents.

Previous research has established the use of DESs for the leaching of Cu and Co from ores and secondary materials [15,24–26]. These studies highlight the ability of DESs to complex metal ions and promote dissolution under relatively mild conditions compared to traditional acids. However, a common limitation in many of these systems is the high viscosity of neat DESs, which restricts mass transfer and thus slows leaching kinetics. To mitigate this, some authors have explored the incorporation of water into DESs to reduce viscosity, but widespread adoption and optimisation remain limited [27,28]. Our work advances this approach by adding 30 wt.% deionised water to choline chloride-based DESs, which not only significantly reduces viscosity and enhances metal–DES interactions but also retains the essential hydrogen-bonding network needed for effective metal complexation and dissolution. This aqueous DES system, combined with the oxidative assistance of H_2O_2, achieves improved leaching efficiencies and kinetics for Cu and Co under moderate temperatures. Thus, our findings provide novel and practical advancement in DES-assisted hydrometallurgy, bridging fundamental solvent chemistry with applied metal extraction processes.

In this study, ChCl was selected as the hydrogen bond acceptor (HBA) for its low cost, non-toxicity, biodegradability, and ability to form stable eutectic mixtures. The hydrogen bond donors (HBDs) were chosen based on their complementary properties: U for its strong hydrogen-bonding capacity and affordability, EG for its high polarity and ability to enhance metal solubility, oxalic acid dihydrate (OA) for its chelating properties and effectiveness in forming stable metal complexes, and thiourea (TU) for its ability to form strong complexes with metals. These selections aimed to optimise the efficiency of leaching Cu and Co from Cu–Co ore. This research is the first to report a comprehensive analysis of the leaching efficiency of these aqueous DESs on Cu–Co ore sourced in the Democratic Republic of Congo (DRC). By comparing the performance of the synthesised DESs with H_2SO_4, this work contributes to understanding how alternative solvents could contribute to sustainable and efficient metal extraction from primary sources.

2. Materials and Methods

2.1. Chemicals

ChCl (≥98.0%), U (99.0%–100.5%), TU (≥99.0%), CuO and CoO (≥99.0%) were purchased from Sigma-Aldrich. EG (≥99.5%) was obtained from Merck. OA dihydrate (≥99.5%), H_2SO_4 (98.0%), and H_2O_2 (50.0%) were purchased from Associated Chemical Enterprise Pty Ltd. All the chemicals were used without any further purification. Deionised water was used to prepare a series of aqueous solutions for all experiments.

2.2. Sample Collection and Preparation

For this investigation, a representative sample of a Cu–Co ore from the DRC was utilised. Homogeneity was achieved by blending about 3 kg of ore, guaranteeing a consistent and representative sample. The material was separated into several size fractions after the ore was reduced in size using a ball mill and a pulveriser. Sieved fractions of −106 + 75, −75 + 53, and −53 + 38 µm were the three main particle sizes into which the ore used for the studies was divided.

2.3. Sample Characterisation

An X-ray fluorescence (XRF) spectrometer (Rigaku NEX DE, Japan) was utilised to determine the elemental composition of the Cu–Co ore. Samples were pulverised, homogenised with a binder, and pressed into pellets to enable accurate quantification of Cu, Co (Table 1), and other elements, thereby identifying both the primary target metals

and potential impurities. Scanning electron microscopy (SEM) was carried out using a Zeiss Sigma high-resolution field emission SEM (FE-SEM SIGMA-03-39), operated with SmartSEM software v6.05, to examine the surface morphology and textural characteristics of the ore and leach residues. Images were acquired in backscattered electron (BSE) mode at an acceleration voltage of 20 kV and an aperture size of 60 mm. Energy dispersive spectroscopy (EDS) was performed using an Oxford Xplore30 detector and Aztec 6.1 SP1 software at a working distance of 12.5 mm, providing complementary elemental data and revealing the distribution of metals and mineral phases at the microscale. Additionally, X-ray diffraction (XRD) analysis was conducted on the Cu–Co ore and leach residues using a Bruker D8 ADVANCE diffractometer with Mo-Kα radiation (λ = 0.710806 Å), operated via DIFFRAC.SUITE EVA v4.2.1. Phase identification was carried out using the PDF-2 RELEASE 2016 RDB database to assess mineralogical changes and phase transformations resulting from the leaching process.

Table 1. Cu–Co ore bulk XRF analysis of Cu–Co Ore sample of different particle sizes.

Particle Sizes (μm)	Composition (Mass %)						
	MgO	Al_2O_3	Fe_2O_3	Co_2O_3	CuO	SiO_2	Others
−53 + 38	3.35	4.85	2.47	0.62	7.53	78.6	2.61
−75 + 53	3.29	4.89	2.21	0.61	7.75	78.8	2.45
−106 + 75	3.30	4.85	2.48	0.59	7.52	78.7	2.59

The term "others" in Table 1 above refers to the collective contribution of minor oxides and trace elements identified in the ore but not listed individually in Table 1. Based on the XRF analysis, these include Na_2O (0.06%–0.08%), P_2O_5 (0.16%–0.19%), SO_3 (0.14%–0.21%), Cl (0.06%–0.07%), K_2O (0.99%–1.05%), CaO (0.31%–0.32%), TiO_2 (0.26%–0.27%), Cr_2O_3 (0.13%–0.30%), MnO (0.13%–0.22%), NiO (0.03%), ZnO (0.01%), ZrO_2 (0.01%–0.02%), and V_2O_5 (0.04%; detected only in the +75–106 μm fraction). These minor minerals could be relevant as they may act as gangue materials or potential contaminants during the leaching process, influencing metal recovery efficiency and the purity of the pregnant leach solution.

2.4. Synthesis of DESs

The four DESs (ChCl:U, ChCl:EG, ChCl:OA, and ChCl:TU) used in this study were synthesised at a 1:1 molar ratio of HBA to HBD. The molar ratio used was based on the previous studies [29–31]. The mixtures were heated and stirred at 70 °C and 400 rpm using a thermostatically controlled heater until a homogeneous, transparent liquid was formed. After preparation, the DESs were allowed to cool to room temperature. The obtained DESs were then kept in a desiccator for 5 days to avoid moisture formation, and before further characterisation using FT-IR. The prepared DESs were vacuum-dried at 65 °C for 24 h. The structures of HBA and HBDs used for the preparation of the DESs are shown in Figure 1.

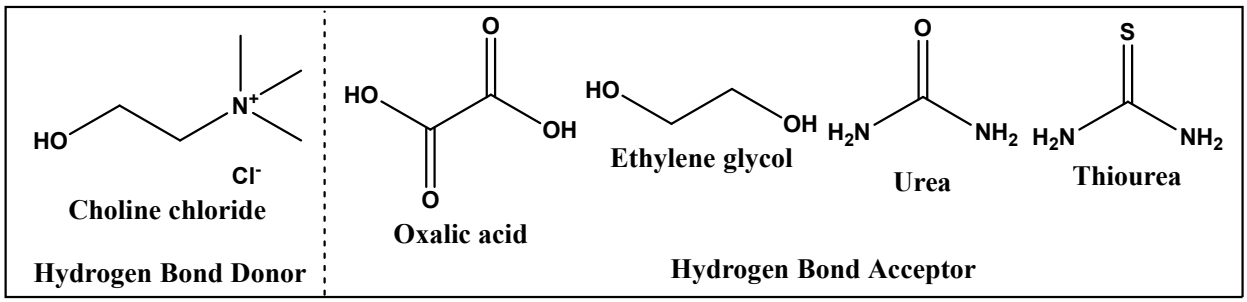

Figure 1. The chemical structures of HBA and HBDs used to prepare DESs.

2.5. Leaching Tests and Analysis

The leaching experiments were conducted using the four synthesised DESs under varying conditions to optimise metal extraction. To enhance their efficiency for leaching applications, 30 wt.% deionised water was added to each prepared DES (it should be noted that a milky solution was observed upon the addition of 30 wt.% water to ChCl:OA DES at room temperature (about 10 °C)). The observed milkiness disappeared at higher temperatures. This addition aimed to reduce the viscosity of the DESs, facilitating better mixing and interaction with the ore particles. This approach is supported by findings from Hammond et al., who demonstrated that most DESs retain their characteristic hydrogen bond network up to a water content of approximately 42 wt.% [27].

The leaching experiments were initially carried out on pure copper (CuO) and cobalt (CoO) oxides at 60 °C for 6 h under 400 rpm agitation at 1:10 solid–liquid ratios (S/L). For the Cu–Co ore leaching, the temperatures investigated were 30 °C, 45 °C, 60 °C, and 75 °C were tested alongside S/L ratios of 1:5, 1:10, and 1:20 in addition to varying the duration of the experiments from 1 h to 8 h at 400 rpm. For comparison, a parallel leaching test using 1 M H_2SO_4 was performed under identical conditions. All experiments were performed in a 250 mL double-neck round-bottom flask, which was placed in a thermostatically controlled shaker equipped with a water bath set to the desired temperature and agitation speed. After leaching, the solutions were filtered through a microfibre filter with a 0.45 µm pore size, and the resulting filtrates were diluted with deionised water before analysis. For experiments involving CuO and CoO, the leachates were diluted 1000-fold, while those from ore leaching were diluted 50 to 100-fold. Atomic absorption spectroscopy (AAS) was performed on the diluted filtrates using an Agilent 200 Series AAS, calibrated with a custom-made multi-element standard obtained from Ultraspec (South Africa). The concentrations of Cu and Co were measured at 327.4 nm and 345.4 nm, respectively. The solid leach residues were thoroughly washed with 50% ethanol, followed by multiple rinses with deionised water, and subsequently dried at 105 °C before further analysis.

To minimise experimental errors, each experiment was repeated twice under the same conditions, and the results were averaged. Leaching efficiency was calculated using Equation (1).

$$Leaching\ Efficiency\ (LE) = \frac{C\,V}{M\,W} \times 100\% \quad (1)$$

In the equation above, C indicates the concentration of metal ions (Cu and Co) in the leachate (g/L) determined using AAS, V represents the volume of the leaching solution (L), M refers to the mass of the Cu–Co ore leached (g), and W indicates the mass percentage of metals of interest in the Cu–Co ore (wt.%) obtained using the XRF.

3. Results and Discussion

3.1. FT-IR Characterisation

The FT-IR spectra of the DESs composed of ChCl with different HBDs (OA, U, TU and EG) used in this study were analysed to confirm their structural interactions. The obtained spectra are shown in Figure 2. For ChCl:OA DES, the broad peak at 3332 cm^{-1} corresponds to O–H stretching, indicative of hydrogen bonding interactions. Peaks at 2879 cm^{-1} and 2558 cm^{-1} represent C–H stretching vibrations from ChCl. The 1725 cm^{-1} peak corresponds to the C=O stretching mode from oxalic acid's carboxyl functional groups, while 1477 cm^{-1} indicates the asymmetric bending vibration of $[N^+(CH_3)_3]$. The 1184 cm^{-1} peak is assigned to the C–O stretching mode, and 951 cm^{-1} corresponds to the asymmetric stretching vibration of $[C–N^+(CH_3)_3]$. The peak at 680 cm^{-1} represents CH_2 rocking vibrations. The presence of C=O and C–O peaks suggests that oxalic acid remains protonated, with strong hydrogen bonding stabilising the DES. For ChCl:U DES, broad peaks

at 3317 cm^{-1} and 3189 cm^{-1} correspond to N–H stretching vibrations characteristic of urea. The 1662 cm^{-1} peak represents the C=O stretching vibration from the amide functional group in urea. Peaks at 1607 cm^{-1} and 1432 cm^{-1} indicate N–H bending vibrations, confirming interactions between choline chloride and urea. The 1165 cm^{-1} peak corresponds to the CH_2 twisting mode, while 1082 cm^{-1} and 952 cm^{-1} represent C–N stretching vibrations from choline chloride. Peaks at 785 cm^{-1} and 523 cm^{-1} are associated with CH_2 rocking and hydrogen bonding interactions, respectively. The shift in N–H and C=O vibrations confirms strong hydrogen bonding in the DES. For ChCl:TU DES, the broad peaks at 3273 cm^{-1} and 3175 cm^{-1} correspond to N–H stretching vibrations. The 1604 cm^{-1} peak represents the C=S stretching mode, characteristic of thiourea. Peaks at 1475 cm^{-1} and 1391 cm^{-1} correspond to N–H bending vibrations, while 1083 cm^{-1} represents the C–N stretching vibration. The peak at 950 cm^{-1} corresponds to asymmetric stretching of [C–$N^+(CH_3)_3$], while 865 cm^{-1} and 734 cm^{-1} indicate CH_2 rocking vibrations. Peaks at 583 cm^{-1} and 470 cm^{-1} are associated with thiourea skeletal vibrations. The shifts in C=S and N–H vibrations confirm strong hydrogen bonding interactions that stabilise the DES. For ChCl:EG DES, the broad O–H stretching peak at 3307 cm^{-1} confirms hydrogen bonding between choline chloride and ethylene glycol. The 2939 cm^{-1} peak corresponds to the C–H stretching vibration, while the 1729 cm^{-1} peak represents the C=O stretching vibration from residual carbonyl groups. The 1478 cm^{-1} peak corresponds to the asymmetric bending mode of [$N^+(CH_3)_3$], and 1193 cm^{-1} and 1038 cm^{-1} represent C–O stretching modes. The 952 cm^{-1} peak corresponds to the C–N stretching vibration, while 862 cm^{-1} represents CH_2 rocking vibrations. The 514 cm^{-1} peak indicates low-frequency vibrations associated with hydrogen bonding. The broad O–H stretching confirms the presence of strong hydrogen bonding, essential for DES stability. Similar FT-IR spectra observations were reported by other authors previously for the investigated DESs [32–34]. The FT-IR spectra confirm the presence of hydrogen bonding in all DESs, with specific functional group interactions stabilising each DES. The shifts in N–H, C=O, C–N, and O–H vibrations indicate strong interactions between ChCl and its respective HBD, forming stable DESs. The vibrations observed in all the synthesised DESs are summarised in Table 2.

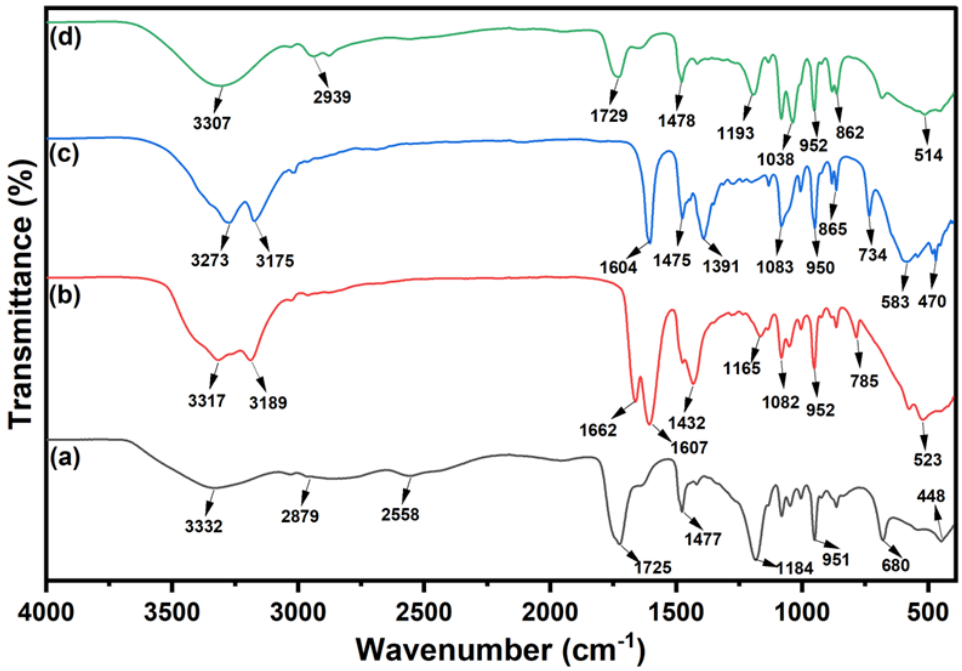

Figure 2. FTIR spectra of (a) ChCl:OA; (b) ChCl:U; (c) ChCl:TU; (d) ChCh:EG DESs.

Table 2. FTIR vibrations observed in the synthesised DESs used in this study.

DESs	Wavenumber (cm^{-1})	Allotment of Regions
ChCl:OA	3332	O–H stretching
	2879, 2558	C–H stretching
	1725	C=O stretching
	1477	$[N^+(CH_3)_3]$ asymmetric bending
	1184	C–O stretching
	951	$[C–N^+(CH_3)_3]$ asymmetric stretching
	680	CH_2 rocking
ChCl:Urea	3317, 3189	N–H stretching
	1662	C=O stretching
	1607, 1432	N–H bending
	1165	CH_2 twisting
	1082, 952	C–N stretching
	785, 523	CH_2 rocking
ChCl:TU	3273, 3175	N–H stretching
	1604	C=S stretching
	1475, 1391	N–H bending
	1083	C–N stretching
	950	$[C–N^+(CH_3)_3]$ asymmetric stretching
	865, 734	CH_2 rocking
ChCl:EG	3307	O–H stretching
	2939	C–H stretching
	1729	C=O stretching (residual)
	1478	$[N^+(CH_3)_3]$ asymmetric bending
	1193, 1038	C–O stretching
	952	C–N stretching
	862	CH_2 rocking

3.2. Screening of Leaching Lixiviants

To determine the most effective aqueous DES solution for Cu and Co dissolution, various DES formulations were evaluated on CuO and CoO. The studied aqueous DES solutions were ChCl:OA, ChCl:EG, ChCl:U, and ChCl:TU. In addition, 1 M H_2SO_4 was included as a benchmark for comparison. The findings revealed considerable differences in leaching efficiencies, with aqueous ChCl:OA DES solution emerging as the top-performing DES, although 1 M H_2SO_4 demonstrated to be the most efficient among all the lixiviants, as depicted in Figure 3. Aqueous ChCl:OA DES solution achieved leaching efficiencies of 89.2% for Cu and 92.4% for Co, outperforming all other DES formulations. Aqueous ChCl:OA DES solution demonstrated the best efficiency because oxalic acid contributes strong acidity and excellent chelating ability, both of which are critical in breaking down metal oxides and forming stable, soluble metal complexes for effective leaching. OA is a dicarboxylic acid and a strong chelating agent. It forms stable complexes with metal ions such as Cu^{2+} and Co^{2+}, due to its two carboxylate groups that can coordinate metal centres. In other words, the low pK_a values of OA (pK_{a1} and pK_{a2} of OA are 1.3 and 4.3, respectively) ensure the availability of protons to disrupt the oxide lattice, making this DES highly effective [35]. Our previous work stressed the importance of pK_a values of acids on the leaching of metals [5]. The study by Pateli et al. further corroborates the best efficiency demonstrated by ChCl:OA DES solution by their finding, which demonstrated that the solubility of metal oxides is higher in DESs with acidic HBDs such as oxalic, lactic, and levulinic acids [18]. This behaviour observed in DESs

with acidic HBDs was linked to the presence of protons (H^+) that act as oxygen acceptors (O^{-2}), which break the metal–oxide bonds.

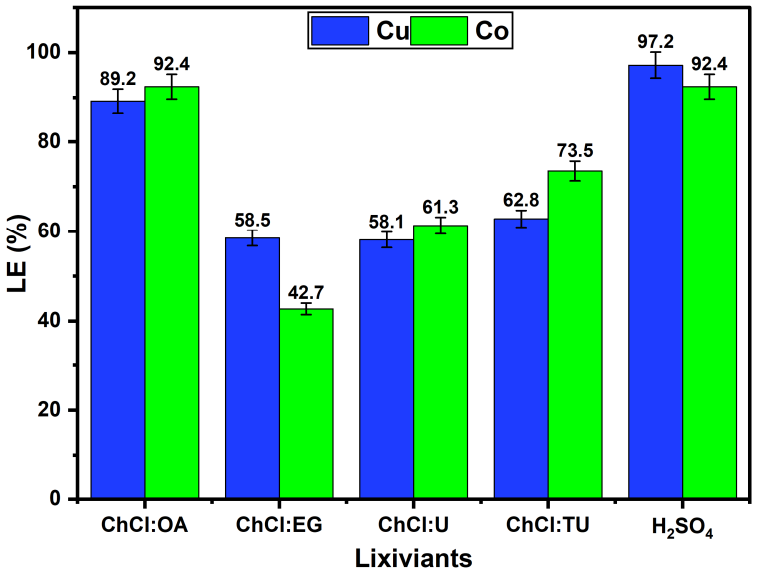

Figure 3. Influence of different lixiviants + 30 wt.% warm water on the leaching of Cu and Co from pure CuO and CoO (t = 6 h, T = 60 °C, agitation speed = 400 rpm, S/L = 1:10).

On the other hand, the ChCl:EG DES solution displayed the lowest leaching efficiencies, achieving only 58.5% for Cu and 42.7% for Co. This underperformance can be attributed to the neutral pH of ChCl:EG DES or the weaker chelating properties of EG (HBD) towards the metal ions [18]. Furthermore, the ChCl:U DES solution achieved moderate metal recovery, with 58.1% for Cu and 61.3% for Co. Although ChCl:U DES, based on urea, offers slightly better coordination through nitrogen donor atoms, but also suffers from low acidity and limited chelating ability, thereby resulting in reduced leaching efficiency. In comparison, the ChCl:TU DES solution showed slightly improved results, recovering 62.8% of Cu and 73.5% of Co. For ChCl:TU DES, incorporating thiourea, has a greater tendency to coordinate metal ions through both sulphur and nitrogen; however, it remains suboptimal for metal oxide dissolution. This could be due to its relatively low acidity and the propensity of its complexes to precipitate or form unstable species.

Previous studies have shown that Cu and Co form chloro complexes in ChCl-based DESs, most especially DESs with low-proton-activity HBDs, such as glycerol, EG, U and TU, among others [36]. For instance, copper demonstrates coordination numbers of approximately 2.4 and 2.5 in ChCl:EG and ChCl:U, respectively, which corresponds to a mixture of $[CuCl_2]^-$ and $[CuCl_3]^{2-}$ species [37–39]. The high chloride ion concentration (about 4.25 M) in systems like EG:ChCl significantly influences speciation, favouring the formation of metal chloro complexes [37]. Spectroscopic investigations, particularly using UV–Vis and EXAFS (extended X-ray absorption fine structure), have confirmed that metal ions in these DESs predominantly exist as tetrachloride complexes, such as $[CuCl_4]^{2-}$ [40]. These findings suggest that metal oxide dissolution in these DESs is driven primarily by a combination of low pH, surface complexation, and ligand exchange processes. This author proposed a generalised reaction mechanism for metal oxide dissolution in DESs, accounting for these factors. In the specific case of CuO and CoO, the formation of $[CuCl_4]^{2-}$ and $[CoCl_4]^{2-}$ (tetrachloridometallate (II) ions) species can be proposed via Equations (2) and (3).

1 M H_2SO_4 achieved the highest leaching efficiencies for the investigated metals, dissolving 97.2% of Cu and 92.4% of Co from the ore, due to its strong acidic properties and ability to release protons that efficiently break down the oxide lattice into soluble

metal sulphates. However, its corrosive nature and environmental drawbacks make it less desirable for sustainable practices. ChCl:OA DES solution was selected for further investigations on Cu–Co ore as it is the most promising alternative solvent among the DESs studied, which offered the highest leaching efficiencies for Cu and Co.

$$CuO_{(s)} + 4Cl^- + 2H^+_{(aq)} \rightarrow CuCl_4{}^{2-}{}_{(aq)} + H_2O_{(l)} \quad (2)$$

$$CoO_{(s)} + 4Cl^- + 2H^+_{(aq)} \rightarrow CoCl_4{}^{2-}{}_{(aq)} + H_2O_{(l)} \quad (3)$$

3.3. Influence of Process Parameters on Cu and Co Leaching from Cu–Co Ore

3.3.1. Particle Size

The particle size significantly influences the leaching efficiency of Cu and Co from Cu–Co ore using ChCl:OA DES + 30 wt.% water at 60 °C, 400 rpm, over 4 h. Among the particle sizes investigated, the −75 + 53 µm range exhibited the highest leaching efficiency, achieving a leaching efficiency of 45.8% for Cu and 55.2% for Co, making it the most effective size under these conditions (Figure 4). In contrast, the smallest particle size (−53 + 38 µm) resulted in leaching efficiencies of 29.7% for Cu and 49.6% for Co, while the largest particle size (−106 + 75 µm) yielded leaching efficiencies of 33.4% for Cu and 48.6% for Co. These results suggest that intermediate particle size balances surface area and diffusion effects more effectively, thereby facilitating higher recovery efficiencies. The effect of particle size on leaching efficiency has been widely discussed in the literature. Studies on Cu leaching kinetics have shown that as particle size decreases, extraction efficiencies often increase due to improved surface area and diffusion effects [41,42]. However, reducing particle size below a specific threshold may yield negligible improvements, as seen in malachite leaching, where the process transitioned to being reaction-controlled for finer particles [9,41]. Therefore, it can be concluded that the leaching efficiency did not strictly increase with decreasing particle size in this study, as might be expected due to the increased surface area of finer particles. This deviation from conventional behaviour may be attributed to particle agglomeration, particularly in the smallest size fractions (−53 + 38 µm), which can reduce the effective surface area exposed to the leaching solution. Similar observations have been reported by other researchers, where fine particles tend to form agglomerates due to surface energy effects, especially under wet conditions, thereby limiting leaching agents' access and diffusion pathways [43,44]. Although agglomeration was not directly assessed in this study, its potential role in influencing leaching kinetics cannot be ruled out and will be considered in future work.

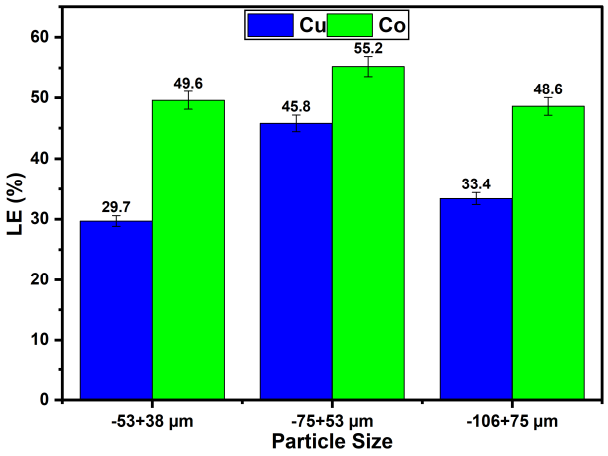

Figure 4. Influence of different Cu–Co particle sizes of ore on the leaching of Cu and Co from a Cu–Co ore using ChCl:OA DES + 30 wt.% warm water (t = 4 h, T = 60 °C, agitation speed = 400 rpm, S/L = 1:10).

3.3.2. Solid-to-Liquid Ratio (S/L)

As illustrated in Figure 5, the S/L ratio significantly influenced the leaching efficiencies of Cu and Co from the Cu–Co ore using the aqueous ChCl:OA DES solution under the specified conditions (t = 4 h, T = 60 °C, agitation speed = 400 rpm, particle size = −75 + 53 µm). It was observed that as the S/L ratio changed from 1:5 to 1:20 (indicating a decrease in the proportion of solid relative to the liquid volume), the leaching efficiencies for both Cu and Co improved remarkably. For instance, at an S/L ratio of 1:5, the leaching efficiencies were relatively low, at 23.1% for Cu and 29.5% for Co. This suggests limited interaction between the ore particles and the DES, likely due to inadequate solvent volume for optimal contact. However, at an S/L ratio of 1:10, the leaching efficiency for Cu rose to 45.8%, and for Co to 55.2%, indicating a notable improvement. This could be attributed to the increased availability of DES for mass transfer and reaction with the ore particles. Interestingly, the highest efficiencies were observed at an S/L ratio of 1:20, where Cu and Co leaching efficiencies reached 88.3% and 84.1%, respectively. The substantial enhancement in leaching efficiency at this ratio can be ascribed to increased interaction between the ore particles and the DES, facilitated by sufficient solvent volume, which promotes efficient mass transfer and complete particle submersion. In other words, a lower solid-to-liquid ratio enhances stirring by reducing diffusional mass transfer resistance and lowering the viscosity of the slurry [45]. However, further increasing the S/L ratio beyond 1:20 could lead to reduced leaching efficiency, potentially due to excessive dilution of the ore in the reaction medium, which diminishes the concentration of active sites for reaction and may lower the overall yield [43].

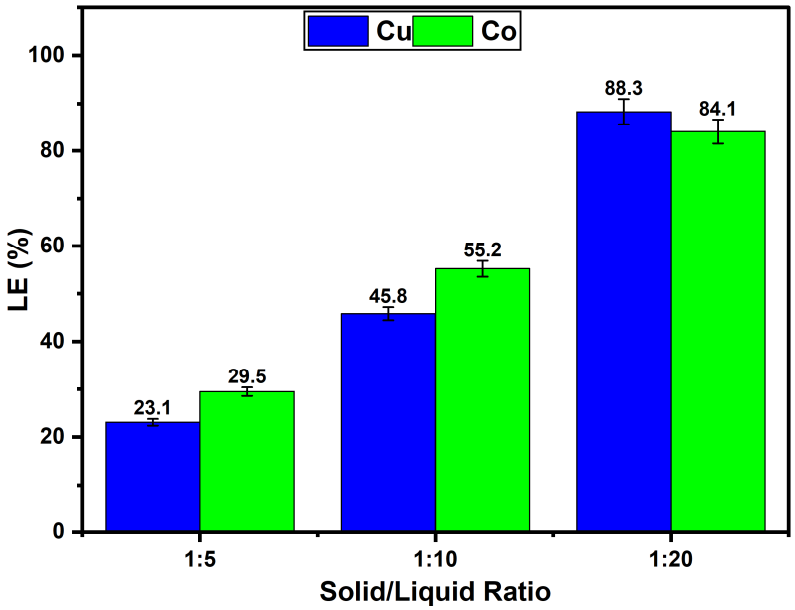

Figure 5. Influence of S/L ratio on the leaching of Cu and Co from a Cu–Co ore using ChCl:OA DES + 30 wt.% water.

3.3.3. Temperature

The influence of temperature on the leaching efficiencies of Cu and Co from a Cu–Co ore using aqueous ChCl:OA DES solution is depicted in Figure 6 under the specified conditions (t = 4 h, agitation = 400 rpm, particle size = −75 + 53 µm, S/L ratio = 1:10). The results indicate that temperature exerts a significant positive effect on the leaching efficiencies of both Cu and Co. As the temperature increased from 30 °C to 75 °C, the leaching efficiency of Cu steadily increased from 16.3% to 71.4%, while the leaching efficiency of Co also increased from 24.8% to 76.7%. This enhancement in leaching efficiency can be

attributed to the increased kinetic energy of reactant molecules at elevated temperatures, which promotes more frequent and effective collisions between the DES and ore particles. Additionally, higher temperatures are likely to reduce the viscosity of the DES, thereby facilitating improved mass transfer and enhanced diffusion of reactants into the solid matrix [5,45]. The temperature-dependent behaviour observed in this study aligns with the general principles of chemical kinetics, where higher temperatures accelerate reaction rates by overcoming energy barriers [46].

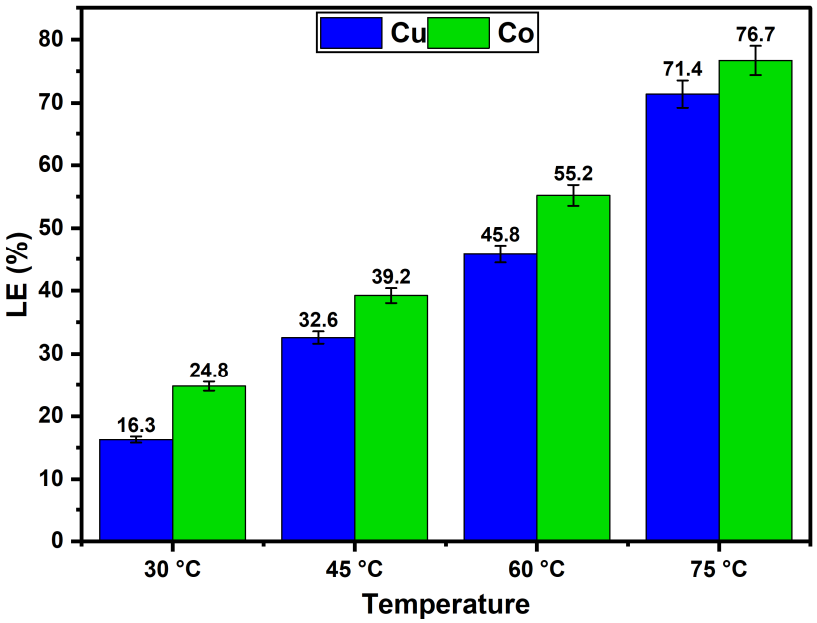

Figure 6. Influence of temperature on the leaching of Cu and Co from a Cu–Co ore using ChCl:OA DES + 30 wt.% warm water.

3.3.4. Contact Time

The effect of leaching time on the leaching efficiencies of Cu and Co from a Cu–Co ore using aqueous ChCl:OA DES solution is presented in Figure 7 under the specified conditions (T = 60 °C, agitation speed = 400 rpm, particle size= −75 + 53 µm, S/L ratio = 1:10). As shown in Figure 7, the leaching efficiencies of both Cu and Co increased significantly with time, reaching maximum values of 85.4% for Co and 79.3% for Cu at 6 h. This trend suggests that extended contact initially enhanced the interaction between the DES and the ore, leading to greater dissolution of both metals. The rapid increase in leaching efficiency during the first 5–6 h reflects the high availability of accessible reactive sites and efficient diffusional transport of the DES components. Interestingly, beyond 6 h, a slight decrease in leaching efficiencies was observed for both Cu and Co, with Cu dropping to 79.1% and Co to 84.9% at 8 h. This slight decrease could be attributed to the potential reprecipitation of metal ions in the solution or the depletion of active leaching agents within the leaching solvents [47]. The diminishing efficiency highlights the potential onset of competing reactions or the stabilisation of equilibrium conditions. Overall, these findings suggest that 6 h is the optimal leaching time for maximum recovery of Cu and Co under the studied conditions, as further prolongation of the process may result in marginal losses in metal extraction efficiency.

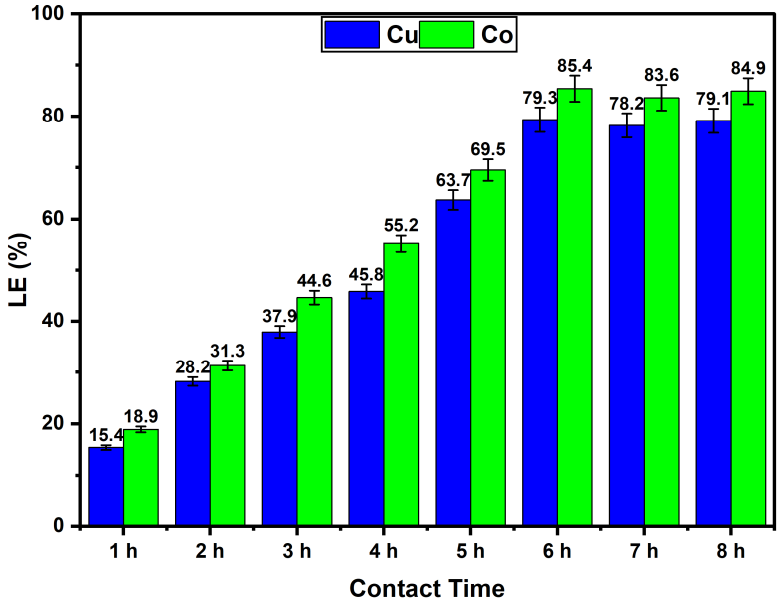

Figure 7. Influence of contact time on the leaching of Cu and Co from a Cu–Co ore using ChCl:OA DES + 30 wt.% warm water.

3.3.5. Different Lixiviants

The effect of different lixiviant systems on the leaching efficiencies of Cu and Co from a Cu–Co ore is presented in Figure 8 under optimised conditions (t = 6 h, T = 75 °C, agitation = 400 rpm, particle size = −75 + 53 µm, S/L ratio = 1:20). The systems investigated include aqueous ChCl:OA DES solution, aqueous ChCl:OA DES solution with the addition of 1 M H_2O_2 as an oxidant, and 1 M H_2SO_4. The aqueous ChCl:OA DES solution achieved notable leaching efficiencies, extracting 92.4% of Cu and 90.6% of Co. The results underscore the effectiveness of aqueous ChCl:OA DES as a lixiviant due to its ability to dissolve Cu and Co-bearing minerals under moderately high-temperature conditions. In addition, incorporating 1 M H_2O_2 into the aqueous DES solution system significantly enhanced the leaching efficiency, yielding 100.0% Cu recovery and 97.5% Co recovery. This improvement can be attributed to the oxidative capabilities of H_2O_2, which generates reactive oxygen species (e.g., hydroxyl radicals and dissolved oxygen) during decomposition, which can oxidise and destabilise metal–oxygen (M–O) bonds in metal oxides. This oxidative attack facilitates the disruption of the oxide matrix and promotes the liberation of Cu^{2+} and Co^{2+} ions into solution. Once released, these metal ions can readily form soluble complexes with the chloride anion from the DES (ChCl:OA) system, further driving the leaching process forward. This dual action, oxidative cleavage of M–O bonds and complexation with coordinating ligands, explains the enhanced recoveries observed [48,49]. Such oxidative dissolution behaviour of metal oxides in H_2O_2-containing systems has been reported in the literature and is particularly effective under elevated temperatures and acidic conditions, as used in this study [48–50]. Furthermore, the reactions involved include the reduction of H_2O_2 to hydroxyl radicals and its decomposition to oxygen (as illustrated in Equations (4) and (5), respectively), which enhances the oxidative dissolution of the target metals. The observed enhancement aligns with findings by Jadhao et al., who reported that the standard reduction potential of H_2O_2 (2.4 V) drives oxidative leaching [51]. Also, Stuurman et al. demonstrated enhanced Co dissolution in similar Cu–Co ores when H_2O_2 was employed, supporting the observed trends in this study [52].

The choice of 1 M H_2O_2 balances efficiency and economic feasibility, avoiding potential side reactions or reagent degradation that may occur at higher concentrations.

$$H_2O_{2(aq)} + 2e \rightarrow 2OH^-_{(aq)} \quad (4)$$

$$2H_2O_{2(aq)} \rightarrow 2H_2O_{(l)} + O_{2(g)} \quad (5)$$

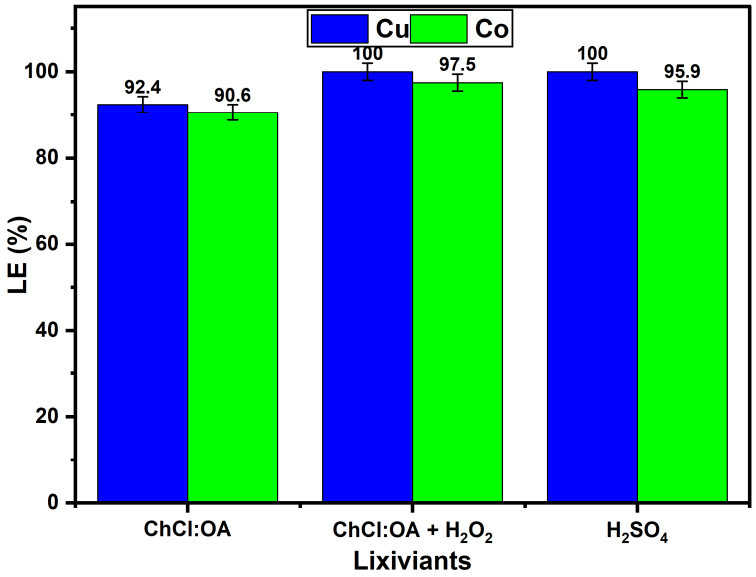

Figure 8. Influence of different lixiviants (aqueous DES solutions and H_2SO_4) on the leaching of Cu and Co from a Cu–Co ore.

In comparison, 1 M H_2SO_4 demonstrated similarly high extraction efficiencies, achieving 100.0% Cu recovery and 95.9% Co recovery. The strong acidic nature of H_2SO_4 promotes the efficient dissolution of metal oxides and sulphides by providing a high proton concentration. However, despite its industrial dominance, the use of H_2SO_4 poses significant environmental and safety concerns, such as corrosivity and the generation of hazardous waste, which limit its suitability for green extraction processes as previously mentioned. In summary, the comparison reveals that the addition of 1 M H_2O_2 to the aqueous solution of ChCl:OA DES system achieves leaching efficiencies comparable to those of H_2SO_4 while offering a more sustainable alternative. The aqueous ChCl:OA + H_2O_2 leaching system thus represents a promising green technology for metal recovery from Cu–Co ores and similar matrices, balancing high efficiency with reduced environmental impact.

The promising leaching efficiencies observed with the aqueous ChCl:OA DES system suggest potential for scale-up and integration into industrial hydrometallurgical processes. The relatively mild operating conditions (60–75 °C, moderate agitation) and use of low-cost, biodegradable components indicate economic and environmental benefits compared to conventional mineral acid leaching. For industrial adaptation, continuous stirred tank reactors or percolation columns could be employed to enhance solid–liquid contact and throughput, leveraging established hydrometallurgical unit operations. Post-leaching, metal recovery from the DES solutions is anticipated to involve established hydrometallurgical techniques such as solvent extraction, precipitation, or electrowinning. Given the strong complexation of Cu and Co species with oxalate and chloride ligands in the DES, selective precipitation or coordinated ligand exchange strategies may be required to recover metals efficiently while enabling DES recycling.

3.4. Dissolution Kinetics

Hydrometallurgical ore processing, a heterogeneous process, requires the interplay of chemical reactions and mass transfer. A heterogeneous reaction can be expressed as R(fluid) + qS(solid) → fluid and/or solid products, where q represents the stoichiometric coefficient of the solid [45]. In the kinetic analysis of leaching, the shrinking-core model (SCM) is widely used to describe non-catalytic heterogeneous reactions [5,53]. The model assumes that the reaction begins at the outer surface of the particle, which is surrounded by a liquid film that enables mass transfer between phases [54]. As the reaction progresses, the reaction front moves inward, leaving behind fully reacted material and inert residue. This creates an unreacted core that gradually shrinks as the reaction continues. A permeable product layer forms around this core, while the original particle size is assumed to remain unchanged throughout the process [54,55]. The leaching behaviour of Cu and Co from a Cu–Co ore in the ChCl:OA + 1 M H_2O_2 solution was evaluated using various SCMs, including the diffusion through the product layer and chemical reaction models. The corresponding mathematical expressions for these models are presented in Equations (6) and (7), respectively. The dissolution kinetics were studied over a range of temperatures (25 °C, 35 °C, 45 °C, 65 °C, and 75 °C) and time intervals (0.5, 1.0, 1.5, 2.0, 2.5, and 3.0 h) using sample with particle size of −75 + 53 µm exposed to an agitation speed of 400 rpm and a 1:20 S/L.

$$1 - 3(1 - X)^{2/3} + 2(1 - X) = k_1 t \quad (6)$$

$$1 - (1 - X)^{1/3} = k_2 t \quad (7)$$

In the equations above, k_1 & k_2 denote rate constants (min^{-1}), t represents time (min), and X symbolises the leached fraction of metal. The Arrhenius equation establishes a correlation between reaction rate constants and temperature, as represented in Equation (8). This relationship is mathematically expressed as:

$$\text{In } k = \text{In } A - E_a/RT \quad (8)$$

Here, k represents the reaction rate constant, A is the pre-exponential factor, E_a denotes the apparent activation energy (kJ mol^{-1}), R is the ideal gas constant ($Jmol^{-1}K^{-1}$), and T is the absolute temperature (K). The E_a can be determined by plotting T^{-1} against ln k and calculating the slope of the resulting linear fit.

In Figure 9, the graph of $1 - 3(1 - X)^{2/3} + 2(1 - X)$ against time at varying temperatures reveals that the data for these metals do not exhibit a perfectly linear relationship. The relatively low correlation coefficients (R^2 values) indicate that the diffusion-controlled shrinking core model (SCM) does not adequately describe the dissolution kinetics for the metals studied. Thus, it can be concluded that the dissolution of Cu and Co is not governed by diffusion-controlled kinetics. Conversely, Figure 10 presents the plot of $1 - (1 - X)^{1/3}$ against time, representing the chemical reaction-controlled model, which shows a significantly better alignment with the experimental data. The higher R^2 values suggest that the rate-determining step is controlled by chemical reactions rather than diffusion. Furthermore, the increasing gradient with temperature implies that higher temperatures enhance leaching efficiency, underscoring the importance of temperature in facilitating the process. Therefore, it can be inferred that the leaching of Cu and Co using aqueous ChCl:OA DES solution is predominantly governed by a chemical reaction-controlled mechanism, with temperature playing a key role in improving the leaching efficiencies of the metals investigated.

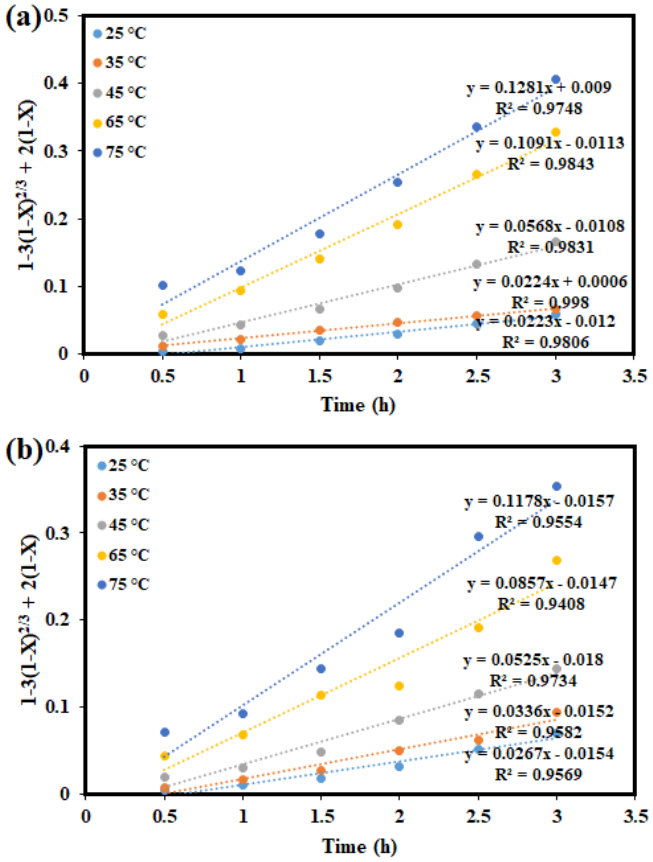

Figure 9. Linear fitting results using the diffusion control model for (**a**) Cu; (**b**) Co.

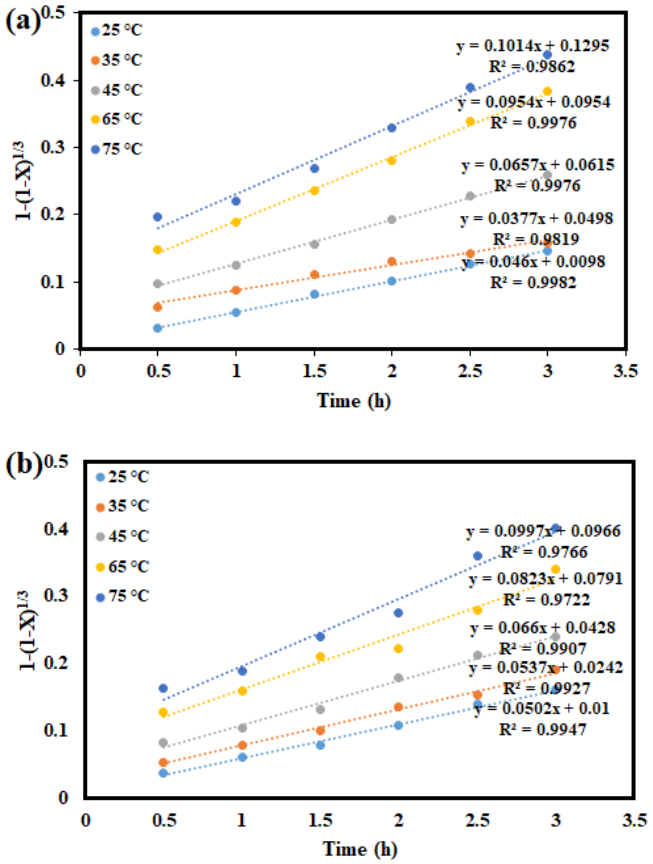

Figure 10. Linear fitting results using the chemical reaction control model for (**a**) Cu; (**b**) Co.

The E_a values obtained for the leaching of Cu and Co from a Cu–Co ore using ChCl:OA solution, as depicted in Figure 11, were determined to be 46.8 kJ mol^{-1} and 51.4 kJ mol^{-1}, respectively, within the temperature range of 25 °C and 75 °C. In addition, the value of R^2 values of the Arrhenius curves for Cu and Co were 0.978 and 0.980, respectively. Typically, E_a for diffusion-controlled processes is below 20 kJ mol^{-1}, while for chemical reaction-controlled processes, it exceeds 42 kJ mol^{-1}. For processes governed by mixed kinetics, the E_a lies between 20 kJ mol^{-1} and 42 kJ mol^{-1} [56]. Since the obtained E_a values exceed 40 kJ mol^{-1}, this indicates that the leaching of Cu and Co is controlled by chemical reactions. This corroborates the findings of the SCM, which also suggests that chemical reactions control the dissolution kinetics of Cu and Co using the ChCl:OA solution. Consequently, increasing the leaching temperature and the concentration of reactants would effectively enhance the leaching efficiency. Previous studies also reported that the rate of a diffusion-controlled process generally exhibits a weak temperature dependence, whereas a chemically controlled process shows a strong sensitivity to temperature variations [5,56,57].

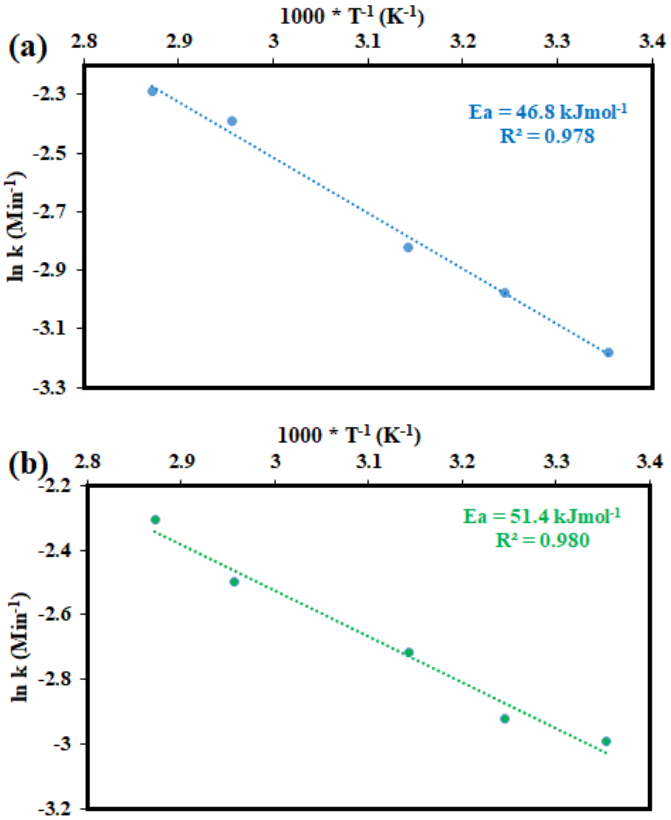

Figure 11. The plots of lnk against 1000/T under $1 - (1 - X)^{1/3}$ for (**a**) Cu; (**b**) Co.

3.5. Characterisation of Pre- and Leached Cu–Co Ore

The residue obtained after leaching Cu and Co from the Cu--Co ore using ChCl:OA DES solution with addition of 1 M H_2O_2 (experimental conditions: t = 6 h, T = 75 °C, agitation = 400 rpm, particle size = −75 + 53 µm, S/L ratio = 1:20) was analysed using SEM and EDS, as shown in Figure 12. These analyses were conducted to evaluate the leaching efficiency and to characterise the changes in the morphology and chemical composition of the sample. The SEM image before leaching reveals a compact and aggregated structure with minimal surface irregularities. The EDS spectrum confirms the presence of significant quantities of Cu (6.2 wt.%) and detectable levels of Co (0.5 wt.%) on the surface, along with other elements such as O (50.9 wt.%), Si (34.7 wt.%), Mg (2.3 wt.%), Al (2.7 wt.%), and Fe (2.1 wt.%). The elevated oxygen content suggests the possible presence of oxides,

while the silica detected might originate from associated gangue minerals. After leaching, the SEM image illustrates a profound transformation in the sample's morphology. The surface appears porous and heavily corroded, characterised by pits and voids, indicative of material dissolution during the leaching process. The corresponding EDS spectrum demonstrates the leaching of the Cu content, reduced to 5.8 wt.%, while Co is reduced to 0.2 wt.%. These results suggest the successful extraction of both Cu and Co. The EDS results also showed that Metals like Mg, Al, and Fe were leached to some extent. However, they are not of interest to us in this study. They will be separated in the future during the separation phase of this project. It should be noted that while EDS provides useful qualitative and semi-quantitative insights, its accuracy for element quantification is limited. It should also be noted that the elemental compositions reported from EDS represent surface-level weight percentages, as EDS is a surface-sensitive technique. These values reflect the relative abundance of elements on the sample surface rather than in the bulk material. The combined SEM-EDS results confirm that the leaching process under the given experimental conditions was effective in extracting Cu and Co, leaving behind a silica-rich residue. The corroded and porous morphology of the residue aligns with the removal of metals from the ore matrix. This characterisation underscores the efficiency of the applied conditions in recovering valuable metals while leaving behind a chemically inert residue.

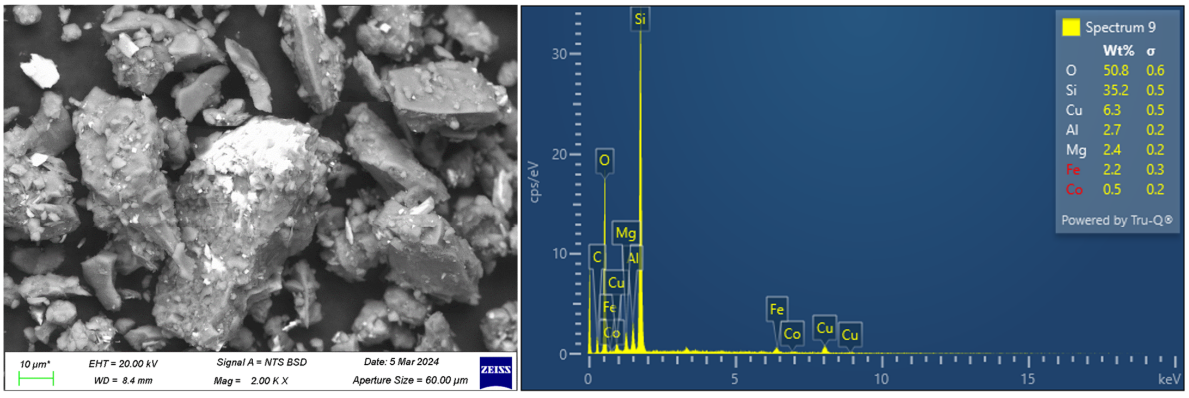

Pre-leached Cu-Co ore sample

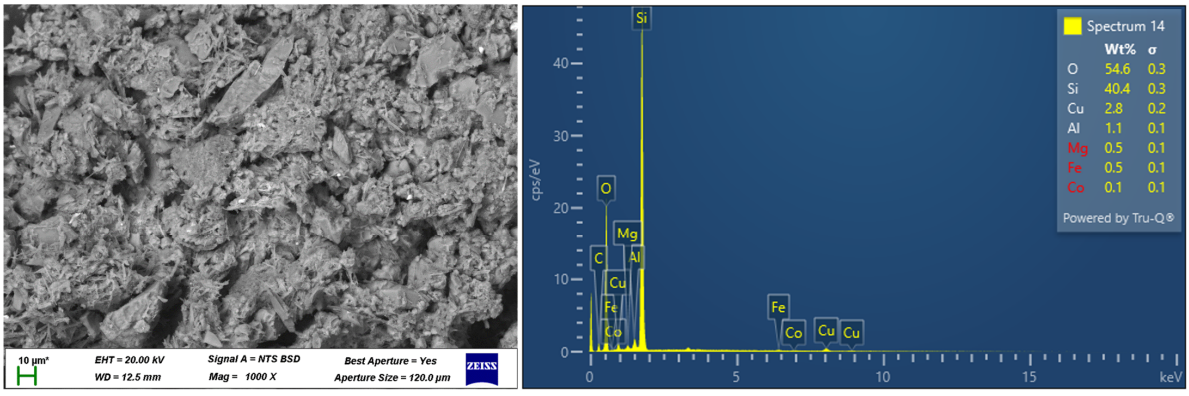

Leached Cu-Co ore sample

Figure 12. Backscattered SEM-EDX images of pre- and leached Cu–Co ore (leaching solvent = ChCl:OA+ 1 M H_2O_2, t = 6 h, T = 75 °C, agitation = 400 rpm, particle size = −75 + 53 µm, S/L ratio = 1:20).

Furthermore, the XRD analysis of the Cu–Co ore before and after leaching with aqueous ChCl:OA DES solution and 1 M H_2O_2 reveals significant mineralogical transformations (Figure 13). The unleached sample is predominantly composed of silicon dioxide (SiO_2, quartz), cobalt (II) oxide (CoO), copper (I) oxide (Cu_2O), cobalt silicate (Co_2SiO_4), and copper cobalt oxide ($CuCo_2O_4$), with SiO_2 being the most prominent phase. Phase identification

was performed using DIFFRAC.SUITE EVA v4.2.1, in conjunction with the PDF-2 RELEASE 2016 RDB database and the corresponding PDF reference codes, are provided in Figure 13. After leaching under optimised conditions (leaching solvent = ChCl:OA + 1 M H_2O_2, t = 6 h, T = 75 °C, agitation = 400 rpm, particle size = −75 + 53 µm, S/L ratio = 1:20), a marked reduction in the intensity of Cu_2O, CoO, and $CuCo_2O_4$ reflections is observed, indicating dissolution of Cu and Co-bearing phases. The persistent and intense reflections of SiO_2 suggest its chemical stability under the leaching conditions. Additionally, the relative intensity reduction in certain peaks implies partial dissolution and structural modification of some residual phases. These results confirm the effectiveness of the aqueous ChCl:OA DES system with 1 M H_2O_2 in leaching Cu and Co, while silicate-based minerals such as quartz remain largely inert. For instance, the persistent presence of cobalt in the silicate phase (Co_2SiO_4) after leaching, as seen in Figure 13, indicates that this fraction remains largely refractory under the applied conditions, representing a minor portion of the total Co content of the investigated ore may require more aggressive treatment for complete dissolution.

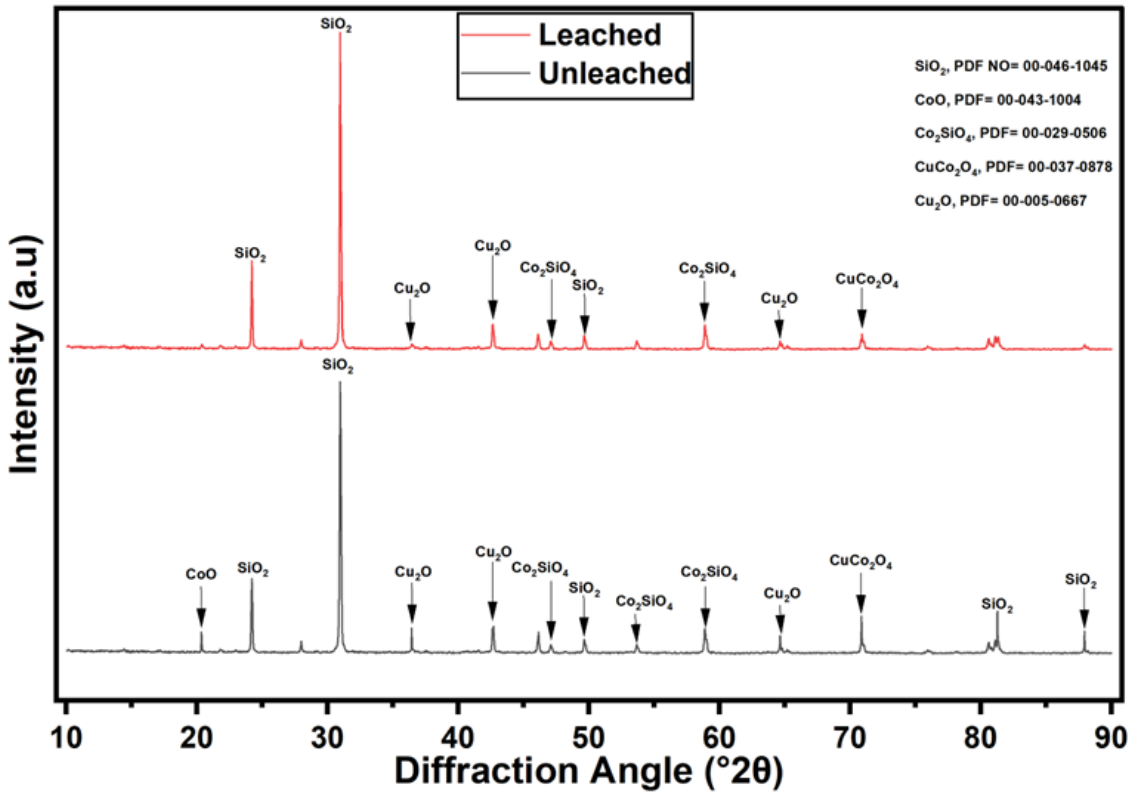

Figure 13. XRD pattern of Cu–Co ore before and after leaching (leaching solvent = ChCl:OA + 1 M H_2O_2, t = 6 h, T = 75 °C, agitation = 400 rpm, particle size = −75 + 53 µm, S/L ratio = 1:20).

4. Conclusions

The study demonstrated the effective leaching of Cu and Co from a Cu–Co ore using various lixiviant systems under optimised conditions. Notably, the ChCl:OA DES solution achieved significant leaching efficiencies, leaching 92.4% of Cu and 90.6% of Co. The addition of 1 M H_2O_2 as an oxidant enhanced these efficiencies to 100.0% for Cu and 97.5% for Co. This improvement underscores the oxidative capabilities of H_2O_2, which facilitates the breakdown of metal-bearing minerals through the generation of reactive oxygen species. Comparatively, 1 M H_2SO_4 also demonstrated high leaching efficiencies, achieving 100.0% Cu and 95.9% Co recovery; however, its environmental and safety drawbacks highlight the advantages of the DES-based systems. The dissolution kinetics were modelled using SCM, revealing that the leaching process was predominantly controlled by surface chemical

reactions. The activation energy values obtained for Cu and Co were 46.8 kJ mol^{-1} and 51.4 kJ mol^{-1}, respectively, which further agrees with the chemical control mechanism and provides a robust framework for scaling up the process. This study demonstrates that ChCl:OA DES solutions provide a sustainable alternative to traditional acidic leaching for Cu and Co recovery. The relatively mild leaching conditions, combined with the use of benign, inexpensive solvents, suggest good potential for scale-up and integration into existing hydrometallurgical operations. The compatibility of DES leaching with known downstream separation techniques, such as solvent extraction and electrowinning, warrants further exploration. Additionally, DES recyclability could reduce operational costs and environmental impacts. Continued development targeting process intensification and metal separation will be critical for realising industrial applicability. Also, future research should focus on refining the process economics, conducting life-cycle assessment, and exploring its applicability to other metal-bearing matrices to broaden its industrial relevance.

Author Contributions: Conceptualisation, E.A.O. and J.H.P.; methodology, E.A.O.; software, E.A.O.; formal analysis, Y.F.; investigation, Y.F.; resources, J.H.P.; data curation, E.A.O.; writing—original draft preparation, E.A.O. and Y.F.; writing—review and editing, E.A.O. and J.H.P.; supervision, E.A.O. and J.H.P.; project administration, J.H.P.; funding acquisition, J.H.P. All authors have read and agreed to the published version of the manuscript.

Funding: This work did not receive any specific funding.

Data Availability Statement: The original contributions presented in this study are included in the article. Further inquiries can be directed to the corresponding author.

Acknowledgments: E.A.O. acknowledges the generous financial support provided to him by the Oppenheimer Memorial Trust (Grant Number: 2024-4758).

Conflicts of Interest: The authors declare that they have no known competing financial interests or personal relationships that could have appeared to influence the work reported in this paper.

Abbreviations

The following abbreviations are used in this manuscript:

DESs	Deep eutectic solvents
ILs	Ionic liquids
HBA	Hydrogen bond acceptors
HBD	Hydrogen bond donors
ChCl	Choline chloride
U	Urea
TU	Thiourea
EG	Ethylene glycol
OA	Oxalic acid dihydrate
DRC	Democratic Republic of Congo
XRF	X-ray fluorescence
SEM	Scanning electron microscopy
EDS	Energy dispersive spectroscopy
XRD	X-ray diffraction
FTIR	Fourier transform infrared spectroscopy
AAS	Atomic absorption spectroscopy
S/L	Solid–liquid ratio
SCM	Shrinking core model
E_a	Activation energy

References

1. Safari, H.; Rezaee, M.; Chelgani, S.C. Ecofriendly Leaching Agents for Copper Extraction—An Overview of Amino and Organic Acid Applications. *Green Smart Min. Eng.* **2024**, *1*, 336–345. [CrossRef]
2. Flores, G.A.; Risopatron, C.; Pease, J. Processing of Complex Materials in the Copper Industry: Challenges and Opportunities Ahead. *JOM* **2020**, *72*, 3447–3461. [CrossRef]
3. Priyam Sharma, J.; Ranjan Sahoo, P.; Mahanta, H.; Venkatesh, A.S.; Babu, E.V.S.S.K.; John, M.M. Constraints on the Genesis of the Proterozoic Bornite Dominated Copper Deposit from Nim Ka Thana, Western India: An IOCG Perspective. *Ore Geol. Rev.* **2020**, *118*, 103338. [CrossRef]
4. Santoro, L.; Tshipeng, S.; Pirard, E.; Bouzahzah, H.; Kaniki, A.; Herrington, R. Mineralogical Reconciliation of Cobalt Recovery from the Acid Leaching of Oxide Ores from Five Deposits in Katanga (DRC). *Miner. Eng.* **2019**, *137*, 277–289. [CrossRef]
5. Oke, E.A.; Potgieter, H.; Mondlane, F.; Skosana, N.P.; Teimouri, S.; Nyembwe, J.K. Concurrent Leaching of Copper and Cobalt from a Copper–Cobalt Ore Using Sulfuric and Organic Acids. *Miner. Eng.* **2024**, *216*, 108853. [CrossRef]
6. Gulley, A.L. One Hundred Years of Cobalt Production in the Democratic Republic of the Congo. *Resour. Policy* **2022**, *79*, 103007. [CrossRef]
7. Alvial-Hein, G.; Mahandra, H.; Ghahreman, A. Separation and Recovery of Cobalt and Nickel from End of Life Products via Solvent Extraction Technique: A Review. *J. Clean. Prod.* **2021**, *297*, 126592. [CrossRef]
8. Długosz, O.; Krawczyk, P.; Banach, M. Equilibrium, Kinetics and Thermodynamics of Metal Oxide Dissolution Based on CuO in a Natural Deep Eutectic Solvent. *Chem. Eng. Res. Des.* **2024**, *202*, 365–376. [CrossRef]
9. Mishra, S.; Ram Jadhao, P.; Pandey, V.; Pant, K.K.; Harbottle, D. Exploring Deep Eutectic Solvents of Methane Sulfonic Acid and Choline Chloride: Formation, Properties, and Metal Solvent Effectiveness. *J. Mol. Liq.* **2024**, *415*, 126338. [CrossRef]
10. Richter, J.; Ruck, M. Synthesis and Dissolution of Metal Oxides in Ionic Liquids and Deep Eutectic Solvents. *Molecules* **2019**, *25*, 78. [CrossRef]
11. Moysiadou, A.; Hu, X. Stability Profiles of Transition Metal Oxides in the Oxygen Evolution Reaction in Alkaline Medium. *J. Mater. Chem. A* **2019**, *7*, 25865–25877. [CrossRef]
12. Di Maria, A.; Merchán, M.; Marchand, M.; Eguizabal, D.; De Cortázar, M.G.; Van Acker, K. Evaluating Energy and Resource Efficiency for Recovery of Metallurgical Residues Using Environmental and Economic Analysis. *J. Clean. Prod.* **2022**, *356*, 131790. [CrossRef]
13. Abbott, A.P.; Frisch, G.; Hartley, J.; Ryder, K.S. Processing of Metals and Metal Oxides Using Ionic Liquids. *Green Chem.* **2011**, *13*, 471. [CrossRef]
14. Chen, W.; Jiang, J.; Lan, X.; Zhao, X.; Mou, H.; Mu, T. A Strategy for the Dissolution and Separation of Rare Earth Oxides by Novel Brønsted Acidic Deep Eutectic Solvents. *Green Chem.* **2019**, *21*, 4748–4756. [CrossRef]
15. Rodriguez Rodriguez, N.; Machiels, L.; Binnemans, K. P-Toluenesulfonic Acid-Based Deep-Eutectic Solvents for Solubilizing Metal Oxides. *ACS Sustain. Chem. Eng.* **2019**, *7*, 3940–3948. [CrossRef]
16. Hansen, B.B.; Spittle, S.; Chen, B.; Poe, D.; Zhang, Y.; Klein, J.M.; Horton, A.; Adhikari, L.; Zelovich, T.; Doherty, B.W.; et al. Deep Eutectic Solvents: A Review of Fundamentals and Applications. *Chem. Rev.* **2021**, *121*, 1232–1285. [CrossRef] [PubMed]
17. Oke, E.A. Examining the Effectiveness of Deep Eutectic Solvents in Removal of Sulfur from Fuel Oil: A Mini Review. *Chem. Afr.* **2024**, *7*, 3565–3578. [CrossRef]
18. Pateli, I.M.; Thompson, D.; Alabdullah, S.S.M.; Abbott, A.P.; Jenkin, G.R.T.; Hartley, J.M. The Effect of PH and Hydrogen Bond Donor on the Dissolution of Metal Oxides in Deep Eutectic Solvents. *Green Chem.* **2020**, *22*, 5476–5486. [CrossRef]
19. Jangir, A.K.; Sethy, P.; Verma, G.; Bahadur, P.; Kuperkar, K. An Inclusive Thermophysical and Rheology Portrayal of Deep Eutectic Solvents (DES) for Metal Oxides Dissolution Enhancement. *J. Mol. Liq.* **2021**, *332*, 115909. [CrossRef]
20. Zinov'eva, I.V.; Fedorov, A.Y.a.; Milevskii, N.A.; Zakhodyaeva, Y.u.A.; Voshkin, A.A. Dissolution of Metal Oxides in a Choline Chloride–Sulphosalicylic Acid Deep Eutectic Solvent. *Theor. Found. Chem. Eng.* **2021**, *55*, 663–670. [CrossRef]
21. Teimouri, S.; Potgieter, J.H.; Billing, C.; Conradie, J. The Feasibility of Pyrite Dissolution in the Deep Eutectic Solvent Ethaline: Experimental and Theoretical Study. *J. Mol. Liq.* **2023**, *392*, 123468. [CrossRef]
22. Zhang, M.; Tian, R.; Han, H.; Wu, K.; Wang, B.; Liu, Y.; Zhu, Y.; Lu, H.; Liang, B. Preparation Strategy and Stability of Deep Eutectic Solvents: A Case Study Based on Choline Chloride-Carboxylic Acid. *J. Clean. Prod.* **2022**, *345*, 131028. [CrossRef]
23. Abbott, A.P.; Boothby, D.; Capper, G.; Davies, D.L.; Rasheed, R.K. Deep Eutectic Solvents Formed between Choline Chloride and Carboxylic Acids: Versatile Alternatives to Ionic Liquids. *J. Am. Chem. Soc.* **2004**, *126*, 9142–9147. [CrossRef]
24. Shiri, H.R.; Mokmeli, M.; Ghadamgahi, S.M.; Babakhani, A. Deep Eutectic Solvents (DESs) for Chalcopyrite Concentrate Extraction: Leaching, Optimization and Kinetics Mechanism. *J. Environ. Chem. Eng.* **2025**, *13*, 117779. [CrossRef]
25. Chen, J.; Zhong, H.; Zhu, S. Study on Cu(II) Extraction Process Optimization and Mechanism from Acidic Leaching Solution Using the Deep Eutectic Solvent P507/Menthol. *J. Mol. Liq.* **2024**, *396*, 123968. [CrossRef]
26. Oke, E.A.; Potgieter, J.H. Sustainable Leaching of Metals from Waste Printed Circuit Boards Using Efficient Carboxylic Acid-Based Deep Eutectic Solvents. *Sep. Purif. Technol.* **2025**, *374*, 133712. [CrossRef]

27. Hammond, O.S.; Bowron, D.T.; Edler, K.J. Structure and Properties of "Type IV" Lanthanide Nitrate Hydrate:Urea Deep Eutectic Solvents. *ACS Sustain. Chem. Eng.* **2019**, *7*, 4932–4940. [CrossRef]
28. Yu, L.; Ji, X.; Xu, X.; Xu, C.; Qi, X.; Wang, G.; Zhang, S.; Cai, J.; Lv, G.; Yang, Z.; et al. Sustainable and Selective Recovery of Copper from Electroplating Sludge via Choline Chloride-Citric Acid Deep Eutectic Solvent: Mechanistic Elucidation and Process Intensification. *Sep. Purif. Technol.* **2025**, *376*, 134195. [CrossRef]
29. Listiana, S.; Bahua, H.; Utami, I.D.; Rahayu, M.D.; Alifah, I.; Kusumaningrum, S. Deep Eutectic Solvent as an Eco-Friendly Catalyst for the Synthesis of Hydroxyphenylglycine Methyl Ester. *IOP Conf. Ser. Earth Environ. Sci.* **2023**, *1201*, 012099. [CrossRef]
30. Moradi, H.; Farzi, N. Experimental and Computational Assessment of the Physicochemical Properties of Choline Chloride/Ethylene Glycol Deep Eutectic Solvent in 1:2 and 1:3 Mole Fractions and 298.15–398.15 K. *J. Mol. Liq.* **2021**, *339*, 116669. [CrossRef]
31. Golysheva, E.A.; Maslennikova, N.A.; Baranov, D.S.; Dzuba, S.A. Structural Properties of Supercooled Deep Eutectic Solvents: Choline Chloride–Thiourea Compared to Reline. *Phys. Chem. Chem. Phys.* **2022**, *24*, 5974–5981. [CrossRef] [PubMed]
32. Shahid, M.; Sahadevan, S.A.; Ramani, V.; Sankarasubramanian, S. Recommended Practices for the Electrochemical Recovery of Cobalt from Lithium Cobalt Oxide: A Case Study of the Choline Chloride:Ethylene Glycol Deep Eutectic Solvent. *ChemSusChem* **2024**, *18*, e202401205. [CrossRef] [PubMed]
33. Lakshmi Papa Rao, G.; Mandal, A.; Pal, N. Choline Chloride-Urea Based Deep Eutectic Solvent: Characterization, Interfacial Behavior and Synergism in Binary (Surfactant) Systems. *Chem. Phys.* **2025**, *588*, 112496. [CrossRef]
34. de Sousa, A.S.; Lima, R.P.; da Silva, M.C.; das Neves Moreira, D.; Pintado, M.M.; de Melo Silva, S. Natural Deep Eutectic Solvent of Choline Chloride with Oxalic or Ascorbic Acids as Efficient Starch-Based Film Plasticizers. *Polymer* **2022**, *259*, 125314. [CrossRef]
35. Kosmulski, M.; Próchniak, P.; Rosenholm, J.B. Surface-Induced Electrolytic Dissociation of Oxalic Acid in Polar Organic Solvents. *Langmuir* **2010**, *26*, 1904–1909. [CrossRef]
36. Aragón-Tobar, C.F.; Endara, D.; de la Torre, E. Dissolution of Metals (Cu, Fe, Pb, and Zn) from Different Metal-Bearing Species (Sulfides, Oxides, and Sulfates) Using Three Deep Eutectic Solvents Based on Choline Chloride. *Molecules* **2024**, *29*, 290. [CrossRef]
37. Hartley, J.M.; Ip, C.-M.; Forrest, G.C.H.; Singh, K.; Gurman, S.J.; Ryder, K.S.; Abbott, A.P.; Frisch, G. EXAFS Study into the Speciation of Metal Salts Dissolved in Ionic Liquids and Deep Eutectic Solvents. *Inorg. Chem.* **2014**, *53*, 6280–6288. [CrossRef]
38. Carlesi, C.; Harris, R.C.; Abbott, A.P.; Jenkin, G.R.T. Chemical Dissolution of Chalcopyrite Concentrate in Choline Chloride Ethylene Glycol Deep Eutectic Solvent. *Minerals* **2022**, *12*, 65. [CrossRef]
39. Tang, J.; Xu, C.; Zhu, X.; Liu, H.; Wang, X.; Huang, M.; Hua, Y.; Zhang, Q.; Li, Y. Anodic Dissolution of Copper in Choline Chloride-Urea Deep Eutectic Solvent. *J. Electrochem. Soc.* **2018**, *165*, E406–E411. [CrossRef]
40. Alabdullah, S.S. PH Measurements in Ionic Liquids. Ph.D. Thesis, University of Leicester, Leicester, UK, 2018.
41. Tanda, B.C.; Oraby, E.A.; Eksteen, J.J. Kinetics of Malachite Leaching in Alkaline Glycine Solutions. *Miner. Process. Extr. Metall.* **2021**, *130*, 16–24. [CrossRef]
42. Tanda, B.C.; Eksteen, J.J.; Oraby, E.A.; O'Connor, G.M. The Kinetics of Chalcopyrite Leaching in Alkaline Glycine/Glycinate Solutions. *Miner. Eng.* **2019**, *135*, 118–128. [CrossRef]
43. Zhang, D.; Dong, L.; Li, Y.; Wu, Y.; Ma, Y.; Yang, B. Copper Leaching from Waste Printed Circuit Boards Using Typical Acidic Ionic Liquids Recovery of E-Wastes' Surplus Value. *Waste Manag.* **2018**, *78*, 191–197. [CrossRef]
44. Zhu, N.; Xiang, Y.; Zhang, T.; Wu, P.; Dang, Z.; Li, P.; Wu, J. Bioleaching of Metal Concentrates of Waste Printed Circuit Boards by Mixed Culture of Acidophilic Bacteria. *J. Hazard. Mater.* **2011**, *192*, 614–619. [CrossRef] [PubMed]
45. Nnanwube, I.A.; Onukwuli, O.D.; Ezekannagha, C.B. Kinetics of Sphalerite Dissolution for Potential Zinc Recovery via Oxidative Leaching. *Can. Metall. Q.* **2024**, *63*, 1592–1603. [CrossRef]
46. Oke, E.A.; Potgieter, H. Recent Chemical Methods for Metals Recovery from Printed Circuit Boards: A Review. *J. Mater. Cycles Waste Manag.* **2024**, *26*, 1349–1368. [CrossRef]
47. Li, X.; Zhao, L.; Chen, S.; Lin, Y.; Hu, X.; Zi, F. Highly Efficient and Selective Extraction of Au(I) from Thiosulfate Gold-Leaching Solution Using Diphenylphosphine. *J. Environ. Chem. Eng.* **2024**, *12*, 111750. [CrossRef]
48. Sokić, M.; Marković, B.; Stanković, S.; Kamberović, Ž.; Štrbac, N.; Manojlović, V.; Petronijević, N. Kinetics of Chalcopyrite Leaching by Hydrogen Peroxide in Sulfuric Acid. *Metals* **2019**, *9*, 1173. [CrossRef]
49. Du, T.; Vijayakumar, A.; Desai, V. Effect of Hydrogen Peroxide on Oxidation of Copper in CMP Slurries Containing Glycine and Cu Ions. *Electrochim. Acta* **2004**, *49*, 4505–4512. [CrossRef]
50. Motasim, M.; Aydoğan, S.; Ali, B.; Agacayak, T. Rotating Disc Method to Study the Dissolution Kinetics of Copper Metal in Citric Acid and Hydrogen Peroxide. *Hydrometallurgy* **2024**, *225*, 106281. [CrossRef]
51. Jadhao, P.R.; Pandey, A.; Pant, K.K.; Nigam, K.D.P. Efficient Recovery of Cu and Ni from WPCB via Alkali Leaching Approach. *J. Environ. Manag.* **2021**, *296*, 113154. [CrossRef]
52. Stuurman, S.; Ndlovu, S.; Sibanda, V. Comparing the Extent of the Dissolution of Copper-Cobalt Ores from the DRC Region. *J. S. Afr. Inst. Min. Metall.* **2014**, *114*, 347–349.

53. Astuti, W.; Hirajima, T.; Sasaki, K.; Okibe, N. Comparison of Atmospheric Citric Acid Leaching Kinetics of Nickel from Different Indonesian Saprolitic Ores. *Hydrometallurgy* **2016**, *161*, 138–151. [CrossRef]
54. Kocan, F.; Hicsonmez, U. Leaching Kinetics of Celestite in Nitric Acid Solutions. *Int. J. Miner. Metall. Mater.* **2019**, *26*, 11–20. [CrossRef]
55. Qin, S.; Yin, B.; Zhang, Y.; Zhang, Y. Leaching Kinetics of Szaibelyite Ore in NaOH Solution. *Hydrometallurgy* **2015**, *157*, 333–339. [CrossRef]
56. Ling, Q.; Zhou, S.; Li, B.; Wei, Y.; Dong, H.; Wang, H. Study on the Chlorination Leaching of Gold and Copper from High Gold-Containing Material Based on Variable Stirring Speed. *JOM* **2024**, *77*, 3151–3166. [CrossRef]
57. Hussaini, S.; Tita, A.M.; Kursunoglu, S.; Kaya, M.; Chu, P. Leaching of Nickel and Cobalt from a Mixed Nickel-Cobalt Hydroxide Precipitate Using Organic Acids. *Minerals* **2024**, *14*, 314. [CrossRef]

Disclaimer/Publisher's Note: The statements, opinions and data contained in all publications are solely those of the individual author(s) and contributor(s) and not of MDPI and/or the editor(s). MDPI and/or the editor(s) disclaim responsibility for any injury to people or property resulting from any ideas, methods, instructions or products referred to in the content.